PHYSICAL REVIEW A VOLUME 18, NUMBER 3 SEPTEMBER 1978

Total electron-detachment cross sections for collisions of negative halogen ions and rare gases for energies around threshold

B. T. Smith, W. R. Edwards, III, L. D. Doverspike, and R. L. Champion
Department of Physics, College of William and Mary, Williamsburg, Virginia 23185
(Received 17 May 1978)

The threshold behavior of the absolute total electron-detachment cross section for collisions of Cl^- and Br^- with rare gases has been determined in an ion-beam–gas-target apparatus. The relative collision energies investigated range from below the electron affinity of the halogen up to about 100 eV. For all of the reactants studied, the threshold for detachment is found to occur at about twice the electron affinity of the negative ion. The general features of measurements are in agreement with the ideas of a simple collision model. Upper limits to detachment-rate constants which are based upon the measurements are presented.

I. INTRODUCTION

In an earlier paper[1] we reported measurements of the absolute total electron detachment and relative elastic differential cross sections for collisions of the negative ion Cl^- with the rare gases Ne, Ar, Kr, and Xe. Those measurements were carried out for relative collision energies which ranged from near the threshold for detachment up to approximately 180 eV. The precise threshold behavior of the total electron-detachment cross section $\sigma(E)$ was difficult to determine in these previous experiments because of the rather large energy spread of the primary ion beam and the inability to obtain sufficiently intense low-energy ion beams. Nevertheless, the experimental results for $\sigma(E)$ were in qualitative agreement with the predictions of a simple complex-potential model, in which the potential parameters were determined from the differential scattering experiments. However, detachment-rate constants derived from those measurements for $\sigma(E)$ were in disagreement with rate constants determined in a shock tube experiment.[2,3]

Measurements of the collisional detachment cross section for relative energies near threshold are important for several reasons. First, such threshold measurements provide essential experimental tests for calculated potential energy curves as well as for models of collisional detachment. Second, collisional detachment and the reverse process (three-body attachment) are important in many areas of physics and chemistry and it is often the relevant rate constants which are of interest. Such rate constants are, of course, strongly dependent upon the detachment threshold.

There have been several studies reported in which the threshold for direct collisional detachment has been investigated extensively. Bydin and Dukel'skii[4] have investigated Br^-, I^- + He, and H_2 and find that the threshold for detachment is greater than the halogen electron affinity for these reactants. Wynn, Martin, and Bailey[5] have measured $\sigma(E)$ down to the threshold for collisions of O^-, O_2^-, and OH^- with He. These authors have also investigated O^- + Ar, Ne as have Roche and Goodyear,[6] but the precise threshold behavior has been difficult to determine experimentally for the latter reactants. Low-energy collisions of O^- with O_2 and other molecular targets have been investigated by Mauer and Schulz,[7] Bailey and Mahadevan,[8] and Roche and Goodyear.[6] For these systems, associative detachment ($X^- + B \rightarrow XB + e^-$) competes with direct collisional detachment at low collision energies, making it difficult to delineate the role of direct detachment.

Experiments which do not use beam techniques but which measure detachment-rate constants directly include flowing afterglow[9] and shock tube experiments.[3,10-12]

The purpose of this paper is to report the results of new experiments in which detailed measurements of the detachment cross section have been made for relative collision energies ranging from below the electron affinity of the negative ion upwards. The systems to be discussed in this paper are

$$Cl^-,\ Br^- + Y \rightarrow Cl,\ Br + Y + e^-,$$

where Y is He, Ne, Ar, and Kr.

II. EXPERIMENTAL APPARATUS AND METHOD

A schematic diagram which illustrates the main features of the apparatus is given in Fig. 1. The apparatus differs somewhat from that described in Ref. 1 in that a different type of ion source has been installed. The negative ion beam is produced by a "surface attachment" ion source which employs a thoriated iridium filament for the active surface. The production of halogen negative ions

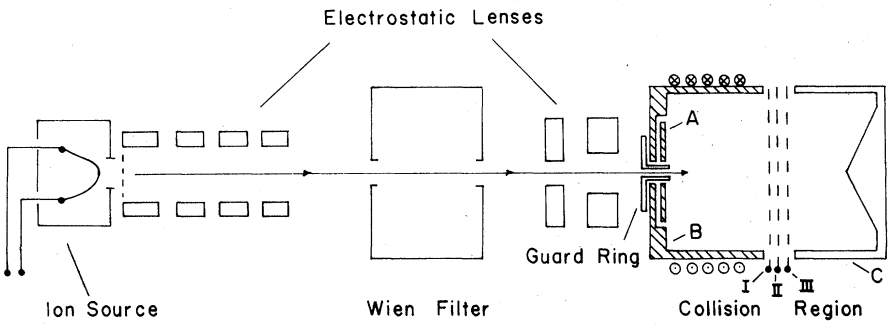

FIG. 1. Schematic diagram of apparatus.

by low work-function hot filaments has been investigated previously[13] and is probably accounted for by a two-step process—molecular decomposition followed by desorption as a negative ion. That is, if R is a compound containing a halogen X then a hot surface may serve as a catalyst for the surface reaction

$$R \rightarrow X + \text{products}. \tag{1}$$

If the electron affinity (EA) of the halogen is greater than the work function of the metal then the probability is high that the halogen desorbs from the surface as a negative ion. The ions are presumably formed very close to the surface, and energy analyses of the ion beam indicate that this is indeed the case. The compounds which work best for producing Cl^- and Br^- are CCl_4 and CBr_4. It should be mentioned that CF_4 (and other fluorinated compounds) were not useful as F^- sources. This is no doubt due to the strong binding of fluorine in compounds, which in turn inhibits the reaction given by Eq. (1).

The ion beam is extracted from the source, focused with electrostatic lens into a Wien filter, and is finally focused into the collision chamber which contains the target gas. This collision chamber, seen in Fig. 1, provides a trap for the detached electrons and has been discussed previously.[1]

The laboratory energy of the primary ion beam can be determined by retarding with grids II and III tied together while monitoring the current to element C. The derivative of the $I_C(V)$ curve yields a curve of approximately Gaussian shape, whose centroid is taken to be the beam energy. For all the total-cross-section experiments reported here, the laboratory energy spread of the primary beam is ~0.60 eV, full width at half-maximum (FWHM). The result of a retardation analysis for a Cl^- ion beam of nominal laboratory energy $E_{Lab} = 6.3$ eV is shown in Fig. 2. Typical currents to the collision chamber range from several tenths of a nanoampere for the lowest laboratory energy (~1 – 2 eV) to several nanoamperes at the highest energy (~2–300 eV).

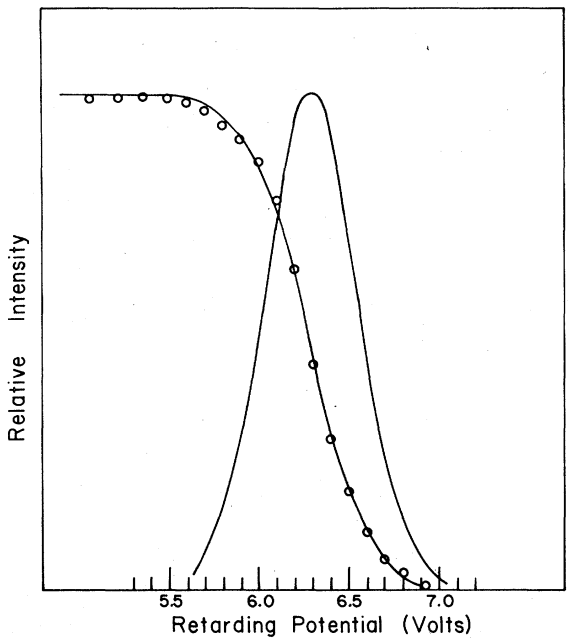

FIG. 2. Retardation analysis used to determine energy distribution of negative ion beam. The open circles are experimental points and an error function which is fitted to these points is shown as a line. The derivative of the error function (a Gaussian function) gives the energy distribution of the primary ion beam.

A. Accuracy: cross section

The detached electrons are collected on element A as a current I_A. Before arriving at element A, some of the detached electrons must pass through grid I twice, causing some absorption of the detached electrons. This absorption has been determined to be $2 \pm 2\%$. Including this correction, the detachment cross section is given by

$$\sigma = -[\ln(1 - 1.02 I_A/I_0)]\,/Nl\,, \tag{2}$$

where I_0 is the primary ion current, l is the reaction path length, and N is the density of scattering centers.

The primary beam current I_0 is determined by completely retarding the primary ion beam with grid I and observing the current to elements A and B of the collision chamber. Both the scattered and primary ion currents (I_A and I_0) are determined by the same digital electrometer. Hence the ratio I_A/I_0 should have no appreciable instrumental error. The pressure of the scattering gas is monitored by an mks capacitance manometer, which appears to have an accuracy of approximately 5%.[14] The effects of thermal transpiration are accounted for when determining the density of scattering centers. The target gas itself is high purity (e.g., 99.998%), and the gas-handling system is designed so that this purity cannot be degraded. In order to remove any trace impurities which are condensible, the target gas is passed through a liquid-nitrogen cooled U tube before entering the collision region. Cross-section measurements at a given energy are always reproducible within a few percent, and do not depend upon the target gas pressure.

The ultimate determination of the accuracy for the measurement of the cross section is, of course, dependent upon whether or not all of the detached electrons (and only electrons) are collected on element A. The magnetic and electrostatic fields of the electron trap are maintained at values where the detected scattered current I_A does not depend upon small variations in the fields. Considering all of the possible sources of error, the experimentally determined cross sections should be accurate within ±10%, except for small cross sections ($\sigma \lesssim 0.2a_0^2$), where the experimental error may constitute a larger percentage of the measurement.

There is one problem that must be discussed further, however. For the situation where the projectile negative ion has an atomic mass less than that of the target species, the laboratory backscattering of the negative ion is possible. This can result in some elastically scattered ions arriving at element A *in addition* to the detached electrons. The effect is usually small and can be accounted for. Otherwise, the measurement for the detachment cross section $\sigma(E)$, will represent an upper limit to that quantity.

B. Accuracy: the energy scale

As discussed earlier, the nominal laboratory energy of the ion beam is determined by a retardation procedure (see Fig. 2). The retarding electric field is provided between grids I and II of the collision chamber. Grid III is electrically connected to grid II during this retardation to assure that there are no electrostatic saddle points through which the ions can pass.

The absolute calibration of the laboratory energy scale is subject to errors associated with surface and contact potentials. Frequent cleanings in addition to careful vacuum procedures are employed to minimize the effects of surface potentials. The inside of the collision chamber is coated with graphite applied in the form of a colloidial suspension. Such graphite coatings have been shown to be useful in minimizing surface variations in contact potentials as well as the contact potential itself.[15] (The maximum contact potential reported in Ref. 15 for graphite-graphite was about 50 mV.)

In an attempt to estimate the magnitude of the uncertainty in the energy scale, the results of two experiments which involved the same reactants but which were performed with deliberately different surface conditions inside the collision chamber[16] have been compared to each other in the region where the total detachment cross section varies most rapidly with energy. The results are shown in Fig. 3, in which the data from the first experiment $\sigma_i(E_i)$ are compared to the second $\sigma_j'(E_j)$. One might expect σ to differ from σ' for two reasons: (i) the cycling of the capacitance manometer to atmospheric pressure is a rather severe operation for a delicate membrane—the calibration of the device may not be completely invariant to such an operation, and (ii) the energy scale may shift due to altered surface or contact potentials. Based on these as-

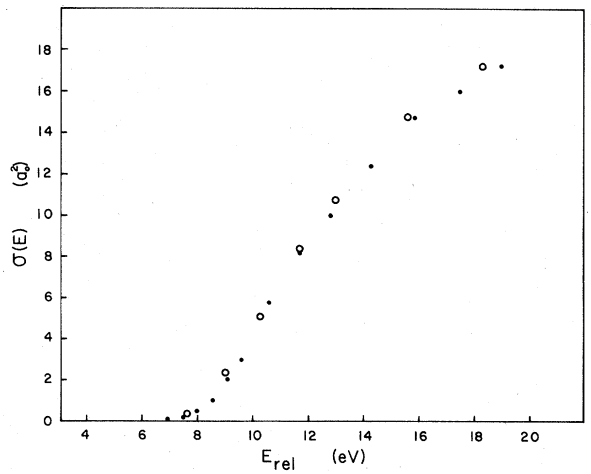

FIG. 3. Results of two different experiments for $Cl^- + Ar$, as discussed in the text. The solid dots are $\sigma_i(E_i)$ and the open circles are $\sigma_j'(E_j)$.

sumptions, the two experiments were compared in the following manner. $\sigma_i(E_i)$ was spline fitted to an analytic function $\sigma(E)$ and the quantity

$$\sum_j |\sigma_j'(E_j) - \beta * \sigma(E_j + \epsilon)|^2 = I(\beta, \epsilon) \quad (3)$$

was minimized by standard numerical codes.[17] $I(\beta, \epsilon)$ was found to be minimized when $\beta = 1.02$ and $\epsilon = 0.064$ eV. This value for ϵ is referred to the c.m. reference frame, implying a possible shift in the laboratory energy scale of approximately 0.12 eV (the reactants were $Cl^- + Ar$). Based upon these findings we feel that it is extremely unlikely that the laboratory energy scale which is determined by our retardation analysis is in error by more than twice this amount, 0.25 eV. The error in the *relative* (c.m.) energy scale is less than this by a factor dependent upon the masses of the reactants, viz.,

$$\Delta E_{\text{rel}} = \Delta E_{\text{lab}} \frac{M_{\text{target}}}{M_{\text{target}} + M_{\text{projectile}}}.$$

III. EXPERIMENTAL RESULTS AND DISCUSSION

The absolute total electron-detachment cross sections for collisions of Cl^- and Br^- with rare gases have been measured for energies ranging from below the threshold for collisional detachment up to laboratory energies of a few hundred eV. The same characteristic dependence of $\sigma(E)$ on relative collision energy is found for each of the systems studied; the cross section rises rapidly from threshold (which is about twice the electron affinity of the negative ion) and tends toward an approximately constant value when the relative energy is sufficiently high. In the discussion which follows we will first examine the threshold region and then the general features of $\sigma(E)$. For the cases where the parameters from a complex potential model exist, calculations will be compared to the experimental results. Finally, rate constants which are determined from $\sigma(E)$ will be presented.

A. Threshold behavior

The experimental results for $Cl^- + Ne$ are given in Fig. 4(a). The relative energy is determined from the laboratory energy by using the average atomic weight of the element (e.g., the mass of Cl^- is taken to be 35.5 amu). This is necessary since the mass resolution of the Wein filter is insufficient to separate the two isotopes of chlorine, Cl^{35} and Cl^{37}.

There are three identifiable sources which cause the true detachment cross section to be broadened or convoluted into the observed results of Fig. 4(a): (i) thermal motion of the target gas; (ii) energy spread of the primary ion beam; and (iii) the

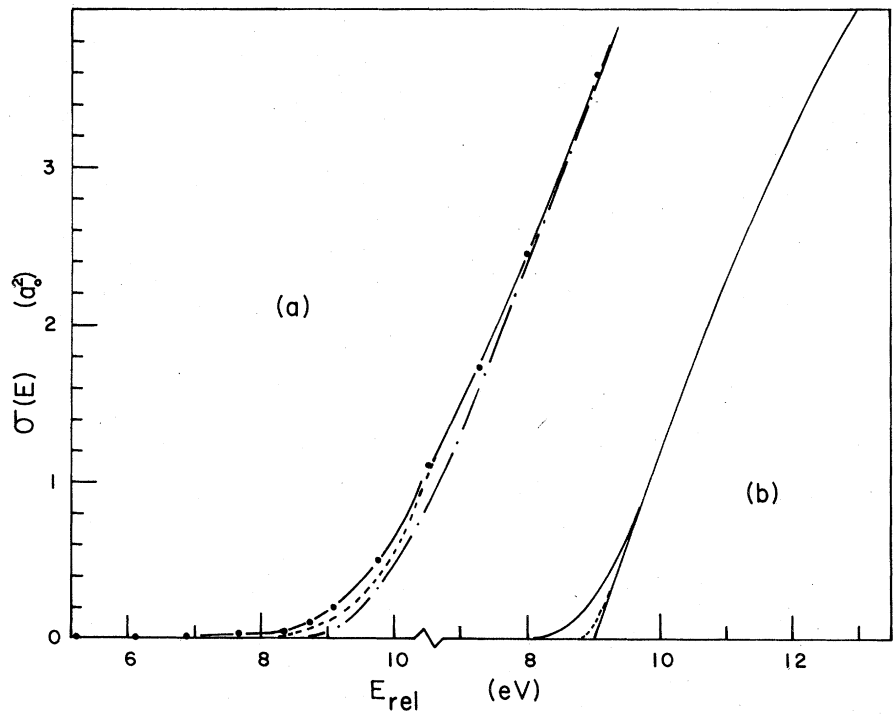

FIG. 4. $\sigma(E)$ for Cl^- + Ne—the solid dots are the experimental measurements and the dashed line is the result of deconvoluting these data. The dot-dashed line is a complex potential calculation for Cl^- + Ne from Ref. 1. (b) An assumed cross-section form given by Eq. (6) and its exact convolution. The dashed line is the result of a numerical deconvolution.

existence of stable isotopes in either the primary ion beam or the target gas. Of these three, (i) is by far the most important and has been discussed in detail by Chantry.[18] If the true detachment cross section is $\sigma_{true}(E)$, where E is the relative energy, then the observed detachment cross section is a result of the convolution

$$\sigma_{obs}(E) = \int G(E' - E)\sigma_{true}(E')\, dE' , \tag{4}$$

where $G(E' - E)$ is an appropriate apparatus function. If $E \gg kT$ then the broadening due to just the thermal motion $G_a(E' - E)$ can be represented by a Gaussian function with a FWHM given by[18]

$$W_a = (11.1\gamma kTE)^{1/2} , \tag{5}$$

where γ is the ratio of the projectile mass to the total mass and T is the temperature of the target gas. Since the effects of broadening are most important in the threshold region, it is reasonable to assume that the width is approximately constant and is given by Eq. (5) with $E \gtrsim E_{th}$ (the threshold energy). For $Cl^- + Ne$, the threshold is about 8 eV, and with $kT = 0.025$ eV, $E = 9$ eV, Eq. (5) yields $W_a = 1.26$ eV.

In order to demonstrate the magnitude of the effects of thermal broadening, let us assume that the true cross section is of the form

$$\begin{aligned} &\sigma_{true}(E') = 0 , \quad E' \leq E_{th} \\ &\sigma_{true}(E') = 10\{1 - \exp[-AE' - E_{th})]\} , \quad E' > E_{th} . \end{aligned} \tag{6}$$

With this form, the convolution integral [Eq. (4)] can be performed exactly [see Eq. (37) of Ref. 18]. The results of such a convolution with $E = 9.0$ eV, $kT = 0.025$ eV, $\gamma = 0.64$, and $A = 0.13$ are shown in Fig. 4(b). It is clear that the inclusion of thermal broadening causes $\sigma_{obs}(E)$ to differ from $\sigma_{true}(E)$ only in the region near the threshold but in that region the effects are important and their neglect could lead to a slight underestimation of E_{th}. This point has been discussed by Chantry.[18]

The laboratory energy spread of the primary ion beam is 0.60 eV, FWHM. Thus, for $Cl^- + Ne$, there is the additional broadening of $\sigma_{true}(E)$ by a convolution function of characteristic width

$$W_b \simeq 0.60(20/55.5) \simeq 0.22 \text{ eV} .$$

The third source of broadening is due to the existence of isotopes in the reactants which causes the mapping of the laboratory data into the c.m. frame of reference to be nonunique. This effect is, however, rather small, and for the systems reported here could cause broadening with a characteristic width $W_c \lesssim 0.15$ eV.

To summarize, the experimental observations are the result of the convolution of $\sigma_{true}(E)$ by an apparatus function whose width is given by

$$W \simeq (W_a^2 + W_b^2 + W_c^2)^{1/2} ,$$

and for $Cl^- + Ne$ $W = 1.3$ eV.

In order to *deconvolute* the experimental results, we have employed a method discussed by Ioup,[19] which uses iterative techniques to solve for $\sigma_{true}(E')$ in the integral equation (4). In order to test the suitability of the deconvolution scheme, the results of the exact convolution already discussed [and shown in Fig. 4(b)] have been treated as experimental data and subjected to the deconvolution procedure. The result of deconvoluting this synthetic data is seen as the dashed line in Fig. 4(b); the agreement with original function is quite good.

The deconvolution procedure of Ioup requires uniformly spaced experimental data which, in our case, were not available. Consequently, an interpolation scheme (Lagrange-Aitken) was used to generate such an array from the experimental data of Fig. 4(a) and this array was then deconvoluted with an apparatus function of width 1.3 eV. The results of the deconvolution differ from $\sigma_{obs}(E)$ only for E near threshold, and those results are shown as a dashed line in Fig. 4(a).

The result of a calculation for $Cl^- + Ne$ which uses a complex potential model and potential parameters from Ref. 1 is also shown in Fig. 4(a). The agreement with the experimental results is seen to be good.

The detachment cross sections for other reactants (for which the mass of the negative ion is greater than the target atom) are shown in Figs. 5 and 6. The effects of numerical deconvolution

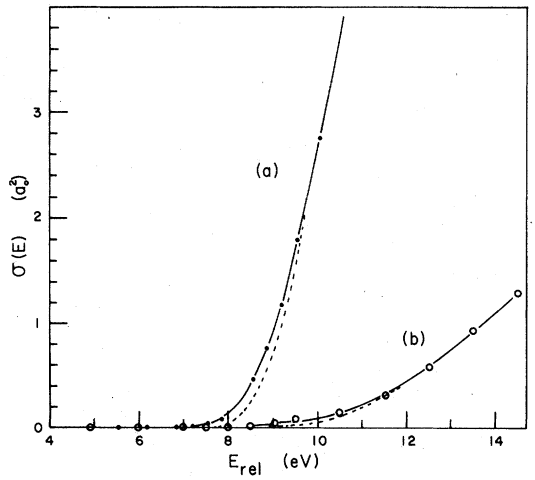

FIG. 5. (a) $\sigma(E)$ for $Br^- + Ar$. (b) $\sigma(E)$ for $Br^- + Ne$. The dashed lines are the results of deconvolution.

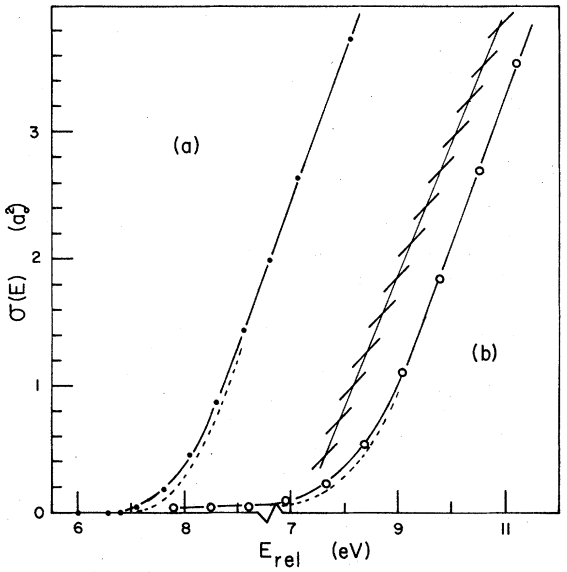

FIG. 6. (a) $\sigma(E)$ for $Cl^- + He$. (b) $\sigma(E)$ for $Br^- + He$. The dashed lines are the results of deconvolution and the crossed line is taken from Ref. 4 for $Br^- + He$.

are seen as dashed lines in these figures. In the case of $Br^- + He$, previous measurements of Bydin and Dukel'skii[4] are compared to the present results in Fig. 6(b) and the agreement is fairly good.

A close inspection of Fig. 6(b) reveals that the detachment cross section for $Br^- + He$ does not approach zero as closely for $E \lesssim 7$ eV as does, e.g., the detachment cross section for $Cl^- + He$. An enlargement of Fig. 6(b) for the $Br^- + He$ reactants is given in Fig. 7. In addition to the predominant threshold observed at $E \sim 7$ eV, there is a lower energy threshold for detachment at the electron affinity of bromine (3.4 eV), which is followed by a plateau region [where $\sigma(E) \simeq 0.06 a_0^2$] which extends up to the predominant threshold. No such effect could be observed for any other reactants. It is possible, of course, that such a region exists for other reactants but the cross section is too small to be measured in our apparatus. This lower limit is about $(0.002-0.005) a_0^2$, depending upon the particular reactants. It should be pointed out that the nature of the laboratory-to-c.m. transformation makes it highly improbable that contaminants cause this plateau effect observed for $Br^- + He$.

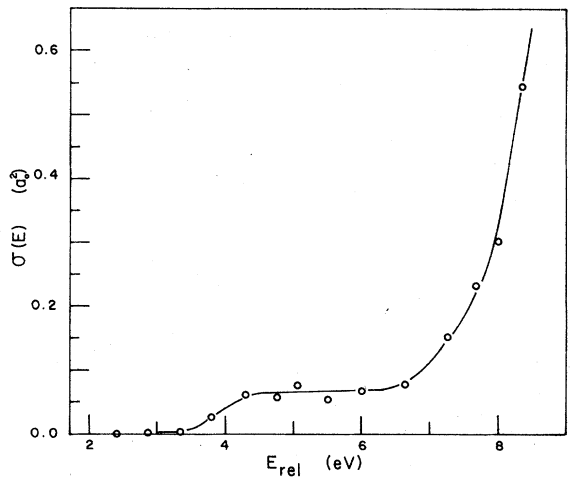

FIG. 7. Details of the low-energy behavior of $\sigma(E)$ for $Br^- + He$.

Three of the systems studied involve collisions of "light-on-heavy" reactants—$Cl^- + Ar$, $Cl^- + Kr$, and $Br^- + Kr$. For these systems laboratory elastic backscattering is possible and, as mentioned in Sec. II, causes the apparent detachment cross section to be too high. This effect is demonstrated in Fig. 8(a) for the above reactants. In contrast to $Br^- + He$, this residual signal does not go to zero at the electron affinity (EA) of the halogen. This apparent cross section $Q_A(E)$ continues smoothly for $E < EA$ and is the sum of the detachment cross section and an elastic backscattering contribution $Q_{BS}(E)$, i.e.,

$$Q_A(E) = \sigma(E) + Q_{BS}(E).$$

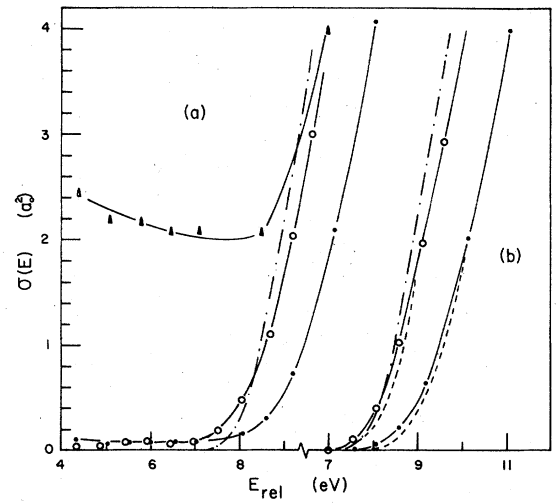

FIG. 8. (a) Apparent cross section $Q_A(E)$ as discussed in text. Triangles—$Cl^- + Kr$; open circles—$Cl^- + Ar$; solid dots—$Br^- + Kr$. (b) Corrected detachment cross sections which result from subtracting the estimated backscattering contribution from the data given in (a). The dashed lines are the results of deconvolution. The dot-dashed line is a complex potential calculation for $Cl^- + Ar$, Kr from Ref. 1.

Based upon the experimental results for the previous reactants, it is reasonable to assume that $\sigma(E)$ is approximately zero for $E \lesssim 7.5$ eV and that for this energy range $Q_A(E) \simeq Q_{BS}(E)$.

This assumption may be tested for $Cl^- + Ar$ and $Cl^- + Kr$ since potential parameters exist for these systems.[1] Referring to Fig. 1, let us define the z direction as that of the primary ion beam with $z = 0$ defining the plane of the circular element labeled "A." The elastic backscattering contribution is then given by

$$Q_{BS}(E) \simeq \frac{\pi}{(L - z_0)} \int_{z_0}^{L} b_0^2(E, z)\, dz\,, \tag{7}$$

where L is the total scattering path length, z_0 is the amount by which the guard ring extends beyond $z = 0$, and $b_0(z)$ is determined from the potential by

$$b_0(E, z) \leftarrow \Theta_{c.m.}(E, z) \leftarrow \theta_{lab} = \tan^{-1}(-R_A/z)\,, \tag{8}$$

where R_A is the radius of element A. As an example, for the case of $Cl^- + Ar$,

$$V(R) = 2530 e^{-1.37R}/R \text{ eV} \tag{9}$$

(when R is expressed in a.u.), and for $z = \frac{1}{2}L$,

$$\theta_{lab} = 138^\circ,$$
$$\Theta_{c.m.}(5 \text{ eV}, \tfrac{1}{2}L) \simeq 173^\circ, \tag{10}$$

and

$$b_0(5 \text{ eV}, \tfrac{1}{2}L) \simeq 0.16 \text{ a.u.}$$

For the energy range from 4 to 8 eV, $Q_{BS}(E)$, as calculated from Eq. (7), is found to be approximately constant at $Q_{BS}(E) = 0.10 a_0^2$, which is in excellent agreement with the experimental observations.

For the case of $Cl^- + Kr$, $Q_{BS}(E)$ is calculated to be $Q_{BS}(5 \text{ eV}) = 2.1 a_0^2$ and $Q_{BS}(7 \text{ eV}) = 1.9 a_0^2$. Again, this is in good agreement with the experimental findings. It appears clear that the assumption that the negative current reaching element A is entirely due to elastic backscattering for relative collision energies below about 7.5 eV is reasonable for these light-on-heavy systems. Consequently, the data for $Cl^- + Ar$ and $Br^- + Kr$ have been corrected for this backscattering and are plotted, along with the deconvoluted results, in Fig. 8(b). An upper limit for $\sigma(E)$ is estimated to be $0.01 a_0^2$ in the energy range below the predominant thresholds of Fig. 8(b). No attempt has been made to correct the $Cl^- + Kr$ data.

Also shown in Fig. 8(a) and repeated in Fig. 8(b) is the result of a calculation for $Cl^- + Ar$, which uses the potential parameters of Ref. 1. The calculation for $Cl^- + Kr$ is indistinguishable from that for $Cl^- + Ar$ in the energy range of Fig. 8. The agreement of the calculations with the experimental results is good.

Olson and Liu[20] have calculated potential energy curves for $ArCl^-$ and $ArCl$. They find that the energy of the ionic state becomes degenerate with that of the ground neutral state $[ArCl(X^2\Sigma)]$ at about 10 eV and this occurs at an internuclear separation of $R = 3.45 a_0$. Based upon the premise that the coupling of the ionic state to the neutral state should be quite small for $R > 3.45 a_0$, this "crossing energy" would appear to be about $2\frac{1}{2}$ eV higher than that indicated by the experimental results of Fig. 8(b).

It is difficult to give a precise and unique experimental definition of the threshold energy for collisional detachment. The usual technique for determining such a threshold is to plot the data in some manner so that an approximately linear behavior is exhibited for energies near threshold. The threshold is then determined by extrapolating a fitted straight line to zero cross section. In our case, a plot of $\sqrt{\sigma(E)}$ vs E is nearly linear over the approximate cross-section range of $0.05 \lesssim \sigma(E) \lesssim 4\ a_0^2$, where $\sigma(E)$ is the deconvoluted detachment cross section which, where necessary, has been corrected for backscattering.

Table I indicates the results for the threshold energy when determined by the above method. The indicated uncertainties in these threshold values are due to fitting the straight line $\sqrt{\sigma(E)}$ vs E in addition to the assumed uncertainty in the laboratory energy scale, 0.25 eV.

There are two observable trends for the threshold values: (i) for a given rare gas the threshold for Br^- detachment is higher than that for Cl^- and (ii) for both negative ions the threshold

TABLE I. Threshold values for collisional detachment and upper limits to detachment-rate constants. The rate constants are obtained from Eq. (11) and the experimental cross sections, as discussed in the text. This upper limit, $k^*(T)$, is expressed in units of $10^{-18}\,cm^3\,sec^{-1}$.

System	Threshold (eV)	k^*(4000 K)	k^*(5000 K)
$Cl^- + He$	7.1 ± 0.1	6.0	56
$Cl^- + Ne$	8.1 ± 0.2	1.9	18
$Cl^- + Ar$ [a]	7.3 ± 0.2	14	110
$Br^- + He$	7.4 ± 0.2 [b]	143	1150
$Br^- + Ne$	8.6 ± 0.2	1.5	13
$Br^- + Ar$	7.7 ± 0.2	2.7	23
$Br^- + Kr$ [a]	8.1 ± 0.2	9	70

[a] Based upon measurements which are corrected for elastic backscattering as discussed in text.

[b] Threshold defined by extrapolating linear fit to $\sigma = 0.06 a_0^2$.

values increase for identical ordering of the rare-gas targets.

B. Cross sections at higher energies

The complete experimental results are displayed in Fig. 9 for Cl^- and in Fig. 10 for Br^-. Corrections for broadening are not included in these figures—they are essentially not observable on such a scale. The cross sections for $Cl^- + Ne$, Ar and Kr differ by 3%–8% in the energy range $E \gtrsim 50$ eV from the values reported earlier.[1] The cause of this discrepancy is unclear but it may be due in part to the determination of the scattering gas pressure.[21]

The results for Br^- detachment can be compared to the observations of Bydin and Dukel'skii[4]: Several points have been taken from their figures and plotted on Fig. 10. With the exception of the argon target, the agreement is quite good. It is interesting to note that the cross section for collisional detachment by Ne falls below that for the He target for sufficiently small relative energies, for both Cl^- and Br^-.

Some evidence for structure in $\sigma(E)$ is apparent for those systems in which high relative energies could be attained. This could be due to a signi-

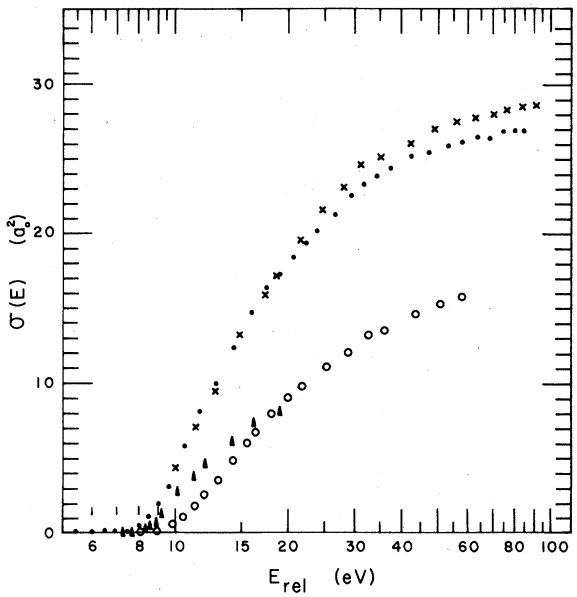

FIG. 9. $\sigma(E)$ for $Cl^- + He$ (triangles), Ne (open circles), Ar (solid dots), and Kr (crosses).

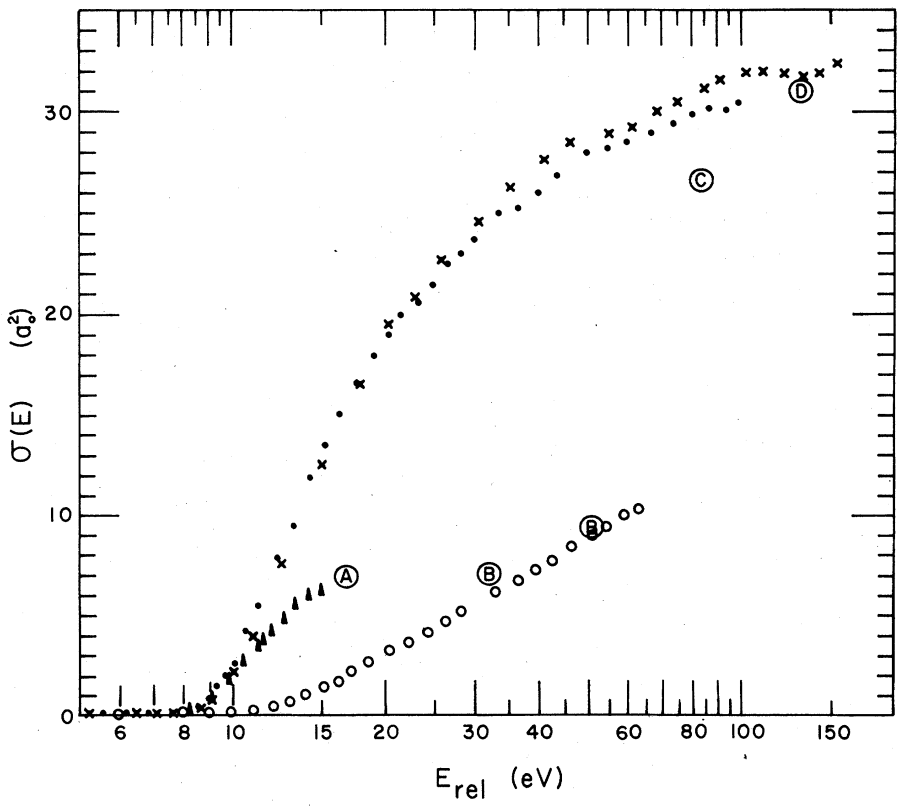

FIG. 10. $\sigma(E)$ for Br^- + He (triangles and Ⓐ), Ne (open circles and Ⓑ), Ar (solid dots and Ⓒ), and Kr (crosses and Ⓓ). The circles which enclose the letters are points taken from Ref. 4.

ficant coupling of the ionic state to excited electronic states of the neutral molecular system.

C. Rate constants

Rate constants for collisional detachment are related to the cross section by the expression

$$k(T) = \frac{0.44*10^{-10}}{(\mu)^{1/2}} (\beta)^{3/2} \int_{EA}^{\infty} E\sigma(E) \exp(-\beta E) dE , \quad (11)$$

where β is $1/kT$ in eV^{-1}, μ is the reduced mass of the reactants expressed in amu, E is the relative collision energy in eV, EA is the electron affinity, and $\sigma(E)$ is expressed in a_0^2. With these units, Eq. (11) gives the rate constant in $cm^3\,sec^{-1}$. Since the threshold for detachment is quite high for the systems studied, it is clear that for temperatures less than about 10 000 K, the detachment rate constants will be very small. An upper limit to this detachment-rate constant can be determined from $\sigma(E)$ by assuming the maximum possible value for $\sigma(E)$, which is consistent with the uncertainty in the measurement. For the example of $Br^- + Ar$, $\sigma_{max}(E) \lesssim 0.003 a_0^2$ for E.A. $\lesssim E \lesssim 5.6$ eV and the cross section rises slowly thereafter until $E \simeq 8$ eV. Some of these details can be seen in Fig. 5. Using these data in Eq. 11, it is found that $k(4500\ K) \simeq 9 \times 10^{-18}\ cm^3\ sec^1$. If the deconvoluted data are used in Eq. (11), the resulting rate constant is obviously smaller. However, the principal contribution to this calculated upper limit for $k(T)$ arises from the low-energy region, where $\sigma(E)$ is determined by the experimental uncertainties. Consequently, it is clear that an upper limit to $k(T)$ is the only meaningful rate constant that can be determined from these experiments. It is plausible that the true rate constant for $Br^- + Ar$ may be less than the above upper limit by a factor of ten or more. Nevertheless, this upper limit for $Br^- + Ar$ is three orders of magnitude smaller than the detachment rate constant for Br^- + Ar reported from shock tube experiments.[3] This discrepancy can in no way be accounted for by uncertainties in the present experiment.

In Table I values of the upper limits for the rate constants computed at $T = 4000$ K and $T = 5000$ K are listed. They have been determined in the same manner as that discussed for $Br^- + Ar$ with no corrections for broadening. The rate constant for $Br^- + He$ is comparatively large due to the observed low-energy plateau in $\sigma(E)$ seen in Fig. 7. For $Cl^- + Ar$ and $Br^- + Kr$, it is necessary to correct for the elastic backscattering in order to calculate $k(T)$. As previously mentioned, it is estimated that $\sigma(E) < 0.01 a_0^2$ for $E \lesssim 7$ eV for these reactants and the rate constants for $Cl^- + Ar$ and $Br^- + Kr$ in Table I are estimates of upper limits for $k(T)$ which are based on this assumption.

The equilibrium rate constant for three-body recombination,

$$X + M + e^- \xrightarrow[k_2(T)]{} X^- + M , \quad (12)$$

is simply related to the detachment-rate constant,

$$X^- + M \xrightarrow[k_1(T)]{} X + M + e^- , \quad (13)$$

by the principle of detailed balance, viz.,

$$k_2(T) = k_1(T)/K(T) , \quad (14)$$

where $K(T)$ is the equilibrium constant. Returning to the example of $Br^- + Ar$, $k_2(T)$ is found to be approximately $1.5 \times 10^{-35}\ cm^6\,sec^{-1}$ at $T = 4000$ K (again an upper limit) when $k_1(T)$ from Table I is used in Eq. (14).

IV. SUMMARY

Detailed measurements of total electron-detachment cross sections for relative energies around the threshold have been made, and for all of the reactants investigated, the predominant detachment threshold is found to be well above the electron affinity of the halogen negative ion. The experimental consequences of broadening, although small, have been removed from the measurements by numerical deconvolution techniques. The experimental results for $Br^- + He$ exhibit a threshold behavior which is not evident for any of the other reactants; the cross section rises from zero at the electron affinity of bromine and remains at an approximately constant small value until the predominant threshold (of about 7 eV) is reached.

The experiments are of sufficient accuracy to serve as meaningful tests for potential calculations and models for collisional detachment. Upper limits for detachment-rate constants—which depend strongly upon the threshold energy—have been determined for some of the reactants studied and are quite small.

Calculations of the detachment cross sections which use previously determined potential parameters of a complex-potential model are found to agree well with the experimental measurements. The experimental results are available in tabulated form and will be supplied upon request.

[1]R. L. Champion and L. D. Doverspike, Phys. Rev. A 13, 609 (1976).
[2]R. L. Champion and L. D. Doverspike, J. Chem. Phys. 65, 2482 (1976).
[3]A. Mandl, J. Chem. Phys. 64, 903 (1976); 65, 2484 (1976).
[4]Iu F. Bydin and V. M. Dukel'skii, Sov. Phys.-JETP 4, 474 (1957).
[5]M. J. Wynn, J. D. Martin, and T. L. Bailey, J. Chem. Phys. 52, 191 (1970).
[6]A. E. Roche and C. C. Goodyear, J. Phys. B 2, 191 (1969).
[7]J. L. Mauer and G. J. Schulz, Phys. Rev. A 7, 593 (1973).
[8]T. L. Bailey and P. Mahandevan, J. Chem. Phys. 52, 179 (1970).
[9]M. McFarland, D. B. Dunkin, F. C. Fehsenfeld, A. L. Schmeltekopf, and E. E. Ferguson, J. Chem. Phys. 56, 2358 (1972).
[10]A. Mandl, B. Kivel, and E. W. Evans, J. Chem. Phys. 53, 2363 (1970).
[11]A. Mandl, J. Chem. Phys. 59, 3423 (1973); 57, 5617 (1972); 54, 4129 (1971).
[12]Von K. Luther, J. Troe, and H. Gg. Wagner, Ber. Bunsenges. Phys. Chem. 76, 53 (1972).
[13]A. Persky, E. F. Green, and A. Kupperman, J. Chem. Phys. 49, 2347 (1968). Also see G. I. Dimov and G. V. Roslyakov, Sov. Phys.-Tech. Phys. 17, 90 (1972); and N. Kashira, E. Vietzhe, and G. Zellerman, Rev. Sci. Instrum. 48, 171 (1977).
[14]This is in accordance with the manufacturer's claims and is also the general observation of W. Frebin, C. Schlier, K. Strein, and E. Teloy, J. Chem. Phys. 67, 5505 (1977). Also see B. Van Zyl, G. E. Chamberlain, and G. H. Dunn, J. Vac. Sci. Technol. 13, 721 (1976).
[15]J. H. Parker and R. W. Warren, Rev. Sci. Instrum. 33, 948 (1962).
[16]The different surface conditions were invoked by coating different regions of the collision chamber with graphite. One experiment was performed just prior to a system cleaning at the termination of a long series of experiments and the other experiment was performed immediately after a system cleaning.
[17]Both routines were from the International Mathematical and Statistical Library—spline fitting with ICSFKU and minimization with ZXSSQ.
[18]P. J. Chantry, J. Chem. Phys. 55, 2746 (1971).
[19]G. E. Ioup and B. S. Thomas, J. Chem. Phys. 46, 3959 (1967); G. E. Ioup, Ph.D. dissertation (University of Florida, 1968) (unpublished). The computer program for the deconvolution was adapted from that given in the latter reference.
[20]R. E. Olson and Bowen Liu, Phys. Rev. A 17, 1568 (1978).
[21]In the period between the measurements of Ref. 1 and the present measurements, the capacitance manometer was returned to the manufacturer for major repair and recalibration.